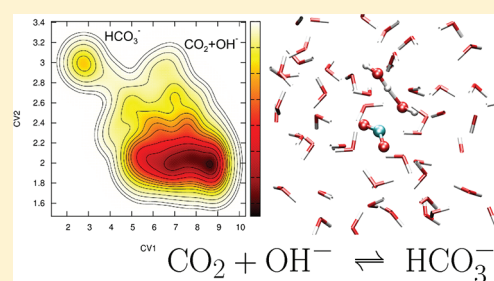


HCO₃[−] Formation from CO₂ at High pH: Ab Initio Molecular Dynamics Study

András Stirling*

Chemical Research Center of the Hungarian Academy of Sciences, Budapest, Hungary

ABSTRACT: Ab initio molecular dynamics simulations have been performed to study the dissolution of CO₂ in water at high pH. The CO₂ + OH[−] → HCO₃[−] forward and the HCO₃[−] → CO₂ + OH[−] reverse paths have been simulated by employing the metadynamics technics. We have found that the free energy barrier along the forward direction is predominantly hydration related and significantly entropic in origin, whereas the backward barrier is primarily enthalpic. The main motifs in the forward mechanism are the structural diffusion of the hydroxyl ion to the first hydration sphere of CO₂, its desolvation, and the C–O bond formation in concert with the CO₂ bending within the hydrate cavity. In the reverse reaction, the origin of the barrier is the rupture of the strong C–O(H) bond. The present findings support the notion that the free energy barrier of the bicarbonate formation is strongly solvation related but provide also additional mechanistic details at the molecular level.



I. INTRODUCTION

The ubiquitous CO₂ and its interaction with water bears enormous significance for the living and nonliving systems of Earth. Hydration of CO₂ plays essential roles in various chemical, biochemical, and geochemical processes in both short and long time scales.¹ CO₂ is also present in living tissues and in biological fluids. In particular, the hydration equilibria and the related kinetics are of vital importance during every respiratory step in the tissues and in the lung capillary vessels. Animals and humans utilize a family of enzymes, the carbonic anhydrases (CAs), to increase the rate of the reversible hydration of CO₂ produced in various ways such as respiration, citrate cycle, or gluconeogenesis.² In these cycles, the enzymes catalyze the reaction of CO₂ with OH[−]



The catalytic effect of these enzymes is a roughly 7 order of magnitude speed up in the reaction rate with respect to the uncatalyzed CO₂ dissolution in water under basic conditions.³ Experimental^{4–7} and theoretical studies^{8–14} have indicated that the origin of this efficiency should be related to desolvation effects. In particular, gas-phase calculations showed barrierless HCO₃[−] formations,^{8–14} while various different explicit hydration models revealed solvent-induced free energy barriers.^{10–14} Although these studies could include many important physicochemical aspects of the alkaline CO₂ dissolution, the definition of the coordinate describing the movement of OH[−] has never captured entirely the mechanism of the OH[−] diffusion. This can affect the free energy estimations because recent studies have shown that the movement of OH[−] in water follows a particular structural diffusion mechanism triggered by the fluctuating local H-bond environment.^{15,16} This implies that a coordinate really collective in nature involving all the water molecules is necessary to describe and boost such

motion. Instead, these earlier simulations have defined an OH[−] ion, and proton transfer from a nearby water molecule was not allowed either by construction^{10–13} or by employing an explicit penalty function.¹⁴ Therefore, in these simulations the hydroxyl anion could only follow a classical diffusive motion.

In this study, we present ab initio molecular dynamics calculations for Reaction 1. We have set out to simulate the elementary steps associated with the forth and back reaction of the above equilibrium using the metadynamics techniques which have been proved to be very efficient in describing rare but reactive events within quantum chemical frameworks.^{17,18} The methodology allows us to use very general reaction coordinates and explore the reaction free energy surfaces (FESs) along these coordinates. Our aim is to gain a detailed mechanistic picture of the hydration of CO₂ at higher pH and explain the origin of the free energy barrier at the molecular level.

II. COMPUTATIONAL DETAILS

The simulation model of the hydrated CO₂ consisted of 63 water molecules and a CO₂ molecule placed into a periodic box of 12.416 × 12.416 × 12.416 Å³. The initial configuration was obtained from classical simulation and was subject to further equilibration for 2 ps with the quantum chemical setup. The molecular dynamics (MD) has been conducted within the Car–Parrinello framework¹⁹ as incorporated into the CPMD program package.²⁰ We have employed the BLYP exchange–correlation functional²¹ and ultrasoft pseudopotentials with a plane wave basis set expanded up to 27 Ry energy cutoff at the Γ point. The hydrogen atoms have been replaced by deuterium which allowed a 7 au time

Received: August 31, 2011

Revised: October 12, 2011

Published: November 04, 2011

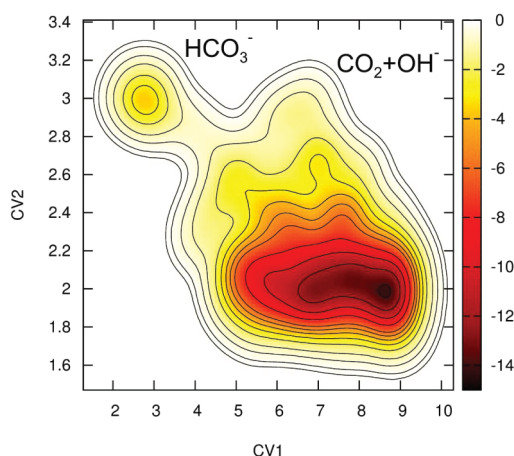


Figure 1. Typical 2D free energy surface (in kcal/mol) for the $\text{CO}_2 + \text{OH}^- \rightarrow \text{HCO}_3^-$ (forward) reaction step as a function of CV1 (distance of the OH^- ion from the carbon atom) and CV2 (coordination number of the carbon atom wrt all oxygens).

step for integrating the MD equations. The fictitious electron mass was 700 au. The same setup has been employed earlier to simulate successfully the neutral CO_2 dissolution in water.²³

To steer the chemical transformations and obtain the underlying FES, we have employed the recently developed metadynamics technique.^{17,22} In metadynamics, we explore the reaction FES as a function of properly selected collective variables (CVs). Usually these CVs correspond to the breaking and forming of bonds, but more general choices are also possible. In the present case, the definition of the hydrated OH^- ion is not obvious due to its diffusion mechanism.^{15,16} We have therefore defined the following coordinate (CV1) to describe the distance between an instantaneous OH^- ion and the carbon atom

$$\text{CV1} = \frac{\sum_{i \in \text{O}_W} d_i \cdot \exp(\lambda n_i^{\text{H}})}{\sum_{i \in \text{O}_W} \exp(\lambda n_i^{\text{H}})} \quad (2)$$

At large negative λ (-20 in the present case) the exponentials select the hydroxyl ion, and the function gives its distance from the CO_2 moiety. d_i is the actual distance between the i th oxygen atom from the carbon, whereas n_i^{H} gives the number of H atoms bonded to this O_i atom

$$n_i^{\text{H}} = \sum_{k \in \text{H}} \frac{1 - \left(\frac{r_{ik}}{r_c}\right)^p}{1 - \left(\frac{r_{ik}}{r_c}\right)^q} \quad (3)$$

where $p = 8$, $q = 32$, and $r_c = 1.27 \text{ \AA}$. This construction is analogous to the coordinate defined for the generalized distance of a hydronium ion from a given atom.²⁵ We have also used the coordination number of the carbon atom with respect to all oxygen atoms (CV2) as expressed in eq 4. This coordinate steers the bond formation between the carbon atom with a nearby oxygen.

$$\text{CV2} = \sum_{i \in \text{O}} \frac{1 - \left(\frac{r_i}{r_c}\right)^p}{1 - \left(\frac{r_i}{r_c}\right)^q} \quad (4)$$

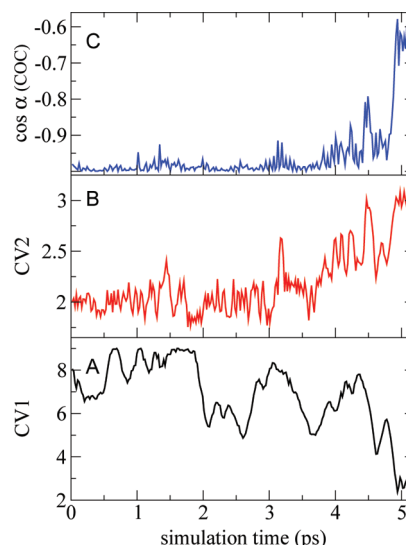


Figure 2. Evolution of CV1 (A, in atomic units), CV2 (B), and the OCO angle (C) during a typical metadynamics simulation of the forward reaction.

Here r_i is the instantaneous distance between oxygen i and the carbon atom. In the forward runs $p = 16$, $q = 32$, and $r_c = 2.0 \text{ \AA}$. For the backward runs, $p = 6$, $q = 14$, and $r_c = 1.8 \text{ \AA}$. The different parametrizations are due to the different chemical situations they describe. The simulations have been therefore performed until the first escape from the reactant free energy well and then continued only for a short period. In other words, the forward and backward steps have been calculated separately.²⁴ For better statistics, multiple runs have been performed. The error of the metadynamics sampling has been estimated to be around 2 kcal/mol ($3k_{\text{B}}T$). Note that the simulations yielded Helmholtz free energies because of the canonical sampling. We assume that within the error of the simulations the experimental Gibbs free energies can be approximated by the corresponding Helmholtz free energies. Additional details of the simulation protocol (in particular, a discussion about the possible error sources and TS verification) can be found in ref 23.

III. RESULTS

For the $\text{CO}_2 + \text{OH}^-$ reaction we have used both CV1 and CV2. The calculated FES is displayed in Figure 1. The calculations yielded a free energy barrier of 13.8 kcal/mol in good agreement with the experimental value of 11.5 kcal/mol.⁷ To understand its molecular origin, the metadynamics trajectories have been analyzed. First we note that the most important structural change in CO_2 activation is the bending of the molecule.²⁶ Figure 2 shows the evolution of both CVs as the simulation proceeds and in parallel the variation of the OCO angle. From Figures 2 and 4 it can be seen that the reaction is concerted but quite asynchronous: first the OH^- ion arrives at the close vicinity of the CO_2 molecule (only CV1 is varying significantly), and then, reaching the TS region, both coordinates change simultaneously. It is also apparent that the variation of CV2 and the bending of the CO_2 molecule nicely correlate, which demonstrates that coordination of a nearby O atom to the CO_2 triggers its bending. A snapshot of the transition state region is shown in Figure 3, where the formation of the C–O bond and the simultaneous bending of CO_2 is captured. The reason for the

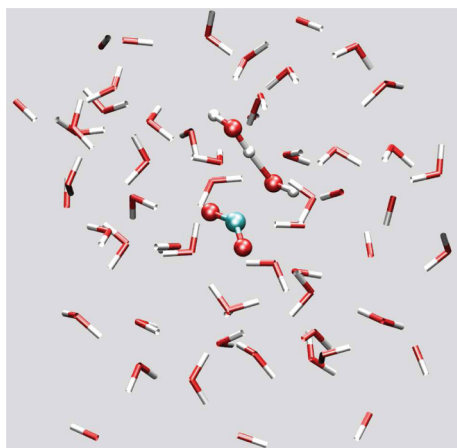


Figure 3. Snapshot of a typical TS configuration. The reaction center (CO_2 + a H-bonded OH^- anion) is highlighted by ball-and-stick representation, while the other water molecules are represented with simple tubes. Fragments are due to the periodic boundary conditions. Fragment H atoms are not shown. Red: O; white: H; blue: C.

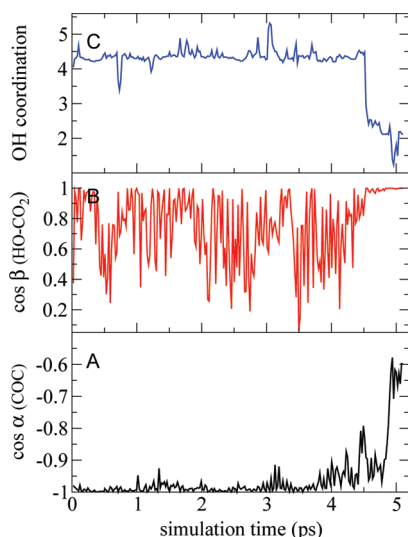


Figure 4. Evolution of the OCO angle (A), the angle between the CO_2 plane and the C–OH axis (B), and the water coordination of the instantaneous OH^- ion²⁹ (C) during a typical metadynamics simulation of the forward reaction.

bending is that the lone pair of the coordinating oxygen atom populates one of the π^* -type degenerate LUMOs of CO_2 . This partial electron transfer breaks the symmetry of CO_2 and induces the bending of the molecule. It is known from earlier simulations²³ that a successful attack by a water molecule from the first hydration shell would require quite high energy (18.8 kcal/mol at this simulation level). This implies that the OH^- attack is far more probable at higher pH.²⁷ Indeed, as the reaction proceeds, we can see that the hydroxyl ion arrives at the first solvation shell²⁸ under the action of the metadynamics potential, and within a picosecond it coordinates to the carbon atom. (Note that due to the bias potential employed for the metadynamics the elapsed time represents only the progress of the simulations but does not correspond to the physical time.) This sequence of events can be clearly seen from Figure 2, at panels A and B.

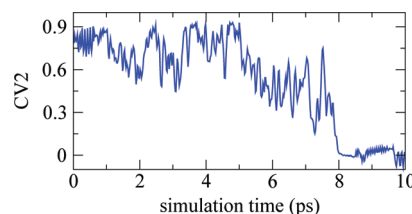


Figure 5. Evolution of CV2 (coordination number of C wrt the hydroxyl O) in the simulation of the backward reaction $\text{HCO}_3^- \rightarrow \text{CO}_2 + \text{OH}^-$.

The coordination at around 4.7 ps is indicated by the rapid decrease in CV1, the saturation in CV2, and the large jump in the OCO bending angle. In fact, the bending angle can serve as a good indicator of the reaction progress.

Further analysis of the trajectories shows that two other structural parameters can also yield information about the details of the mechanism. These are (i) the angle (β) between the direction of the OH^- attack and the CO_2 plane (the molecule is never really linear due to vibrations) and (ii) the number of the coordinating water molecules around the OH^- ion (CN_{OH}).²⁹ They are plotted in Figure 4, along with the evolution of the OCO bending, which serves as a one-dimensional measure for the reaction course. It can be seen that angle β shows remarkable change around and after the TS (panel B in Figure 4). This angle is important because in principle the OH^- ion can arrive from an arbitrary direction with respect to the CO_2 plane, whereas the product HCO_3^- ion is planar apart from thermal fluctuations. Indeed, initially β varies randomly, and it becomes well-defined only when the OH^- anion is close enough to the carbon atom. It was also seen from the trajectories that CN_{OH} changes drastically at the TS region. Initially its value fluctuates around 4 in agreement with the observation that the OH^- ion in water prefers a high coordination state.^{15,31} At around 4.5 ps, CN_{OH} sharply decreases to 2.5. It is important to note that this drop occurs simultaneously with two other characteristic changes: angle β becomes roughly zero (Figure 4, panel B) and the hydroxyl ion gets very close to CO_2 (Figure 2, panel A). These observations indicate that to reach the TS region the OH^- ion has to arrive at the first hydration sphere, where it loses a large part of its hydration sphere. This in turn allows interaction with the CO_2 molecule, and this interaction defines and synchronizes the plane of the CO_2 bending. Since the bending requires room within the hydration sphere, a few water molecules have to be displaced from the immediate vicinity of the CO_2 molecule.³² Within a few hundreds of femtoseconds this can occur, and the reaction takes place completely. In fact from the TS region the reaction is fully analogous to the gas-phase, nonhydrated process which is a barrierless process. The above sequence of events implies that the work to surpass the activation free energy barrier involves the configurational entropy associated with the random migration of the hydroxyl anion (in general, the entropy contribution due to the bimolecularity of the reaction), the activation energy for its transport (ca. 3 kcal/mol),¹⁵ the loss of a couple of H-bonds, and the free energy to displace water molecules at the plane of the bending CO_2 . Hence, similarly to earlier mechanistic proposals,^{8–14} the reaction barrier is attributed to solvent-related effects.

For the reverse reaction ($\text{HCO}_3^- \rightarrow \text{CO}_2 + \text{OH}^-$) the single CV2 has been proved to be sufficient. Indeed, it is seen in Figure 1 that between the TS and the product HCO_3^- regions the two CVs vary strictly concertedly. Hence, at this region any of

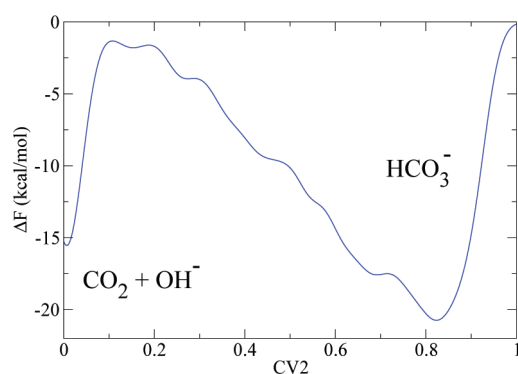


Figure 6. Typical free energy curve along the CV2 reaction coordinate (in kcal/mol) for the $\text{HCO}_3^- \rightarrow \text{CO}_2 + \text{OH}^-$ (backward) reaction step.

them is sufficient to characterize the reaction. The variation of this single CV is displayed in Figure 5, while Figure 6 shows the free energy as a function of CV2 obtained from a typical 1D metadynamics run (until the first arrival at the reactant $\text{CO}_2 + \text{OH}^-$ well). Along the reverse path, the reaction starts with the gradual elongation of the C–O(H) bond, and after reaching the TS region, where the bond length becomes ca. 1.8 Å, on the downhill side of the FES, the hydroxyl anion quickly diffuses away and the hydrated CO_2 molecule forms. The simulations yielded an activation free energy of 20.7 kcal/mol in nice agreement with the 21.5 kcal/mol experimental value.⁷ This barrier is significantly higher than that of the forward reaction. In this case, however, the dominant part of the activation energy is required to break the strong C–O bond, and entropy plays only a limited role. Indeed the chemical change is very localized, and the activation phase of the reaction is confined inside the first hydration sphere. Note that during the reaction the delocalized negative charge of HCO_3^- gradually localizes on the leaving OH group which requires rearrangements in the hydrate sphere, and this necessarily appears also in the barrier.

From the activation free energies of the forward and backward steps, the reaction free energy can be obtained: -6.9 kcal/mol for the equilibrium in eq 1 in good accord with the corresponding experimental -10.0 kcal/mol value. The discrepancy can be attributed to both the error propagation and the inherent limitations of the methodology.²³

The present findings strongly support the notion that the free energy barrier along the $\text{CO}_2 + \text{OH}^- \rightarrow \text{HCO}_3^-$ path is due to various hydration-related effects. Hence, to accelerate the reaction, the catalysts have to target these aspects of the reaction. This can be achieved in various ways, such as preventing the OH^- migration or by desolvating the reactants. In fact, the remarkable acceleration of the CA enzymes^{2,3} has long been attributed to desolvation effects. Our results now provide additional details of the uncatalyzed process and therefore help to understand the key functions enzymes developed to efficiently catalyze CO_2 conversion to bicarbonate in living organisms.

IV. CONCLUSIONS

In this study, we have studied the reaction mechanism of CO_2 dissolution at high pH. The reaction mechanism and the activation free energy barrier of the formation and decomposition of HCO_3^- have been obtained from ab initio metadynamics simulations. It has been found that the reaction barrier along the forward path involves the work of bringing the hydroxyl

anion into the first hydration shell of CO_2 , its dehydration, and the synchronized bending of the CO_2 moiety inside the hydration cavity. Thus, the activation free energy involves significant entropic contributions. In contrast, the decomposition of the bicarbonate anion features a much higher activation free energy barrier which is predominantly enthalpic in origin.

AUTHOR INFORMATION

Corresponding Author

*E-mail: stirling@chemres.hu.

ACKNOWLEDGMENT

This work has been supported by OTKA Grant K68360. A substantial part of the calculations have been performed on the resources of NIIF. We thank Dr. Péter Stefán (NIIF) for technical assistance.

REFERENCES

- (1) Wootton, J. T.; Pfister, C. A.; Forester, J. D. *Proc. Natl. Acad. Sci. U.S.A.* **2008**, *105*, 18848–18853. Feely, R. A.; Sabine, C. L.; Lee, K.; Berelson, W.; Kleypas, J.; Fabry, V. J.; Millero, F. J. *Science* **2004**, *305*, 362–365. Sabine, C. L.; Feely, R. A.; Gruber, N.; Key, R. M.; Lee, K.; Bullister, J. L.; Wanninkhof, R.; Wong, C. S.; Wallace, D. W. R.; Tilbrook, B.; Millero, F. J.; Peng, T.-H.; Kozyr, A.; Onon, T.; Rios, A. F. *Science* **2004**, *305*, 367–371. Heimann, M.; Reichstein, M. *Nature* **2008**, *451*, 289–292. Takahashi, T. *Science* **2004**, *305*, 352–353. Solomon, S.; Plattner, G.-K.; Knutti, R.; Friedlingstein, P. *Proc. Natl. Acad. Sci. U.S.A.* **2009**, *106*, 1704–1709. Lackner, K. L. *Ann. Rev. Energy Environ.* **2002**, *27*, 193–232. Hoegh-Guldberg, O.; Mumby, P. J.; Hooten, A. J.; Steneck, R. S.; Greenfield, P.; Gomez, E.; Harvell, C. D.; Sale, P. F.; Edwards, A. J.; Caldeira, K.; Knowlton, N.; Eakin, C. M.; Iglesias-Prieto, R.; Muthiga, N.; Bradbury, R. H.; Dubi, A.; Hatzioi, M. E. *Science* **2007**, *318*, 1737–1742.
- (2) Lindskog, S. *Pharmacol. Ther.* **1997**, *74*, 1–20. Christianson, D. W.; Fierke, C. A. *Acc. Chem. Res.* **1996**, *29*, 331–339. Silverman, D. N.; McKenna, R. *Acc. Chem. Res.* **2007**, *40*, 669–675.
- (3) Silverman, D. N.; Lindskog, S. *Acc. Chem. Res.* **1988**, *21*, 30–36.
- (4) Pinsent, B. R. W.; Pearson, L.; Roughton, F. J. W. *Trans. Faraday Soc.* **1952**, *56*, 1512–1520.
- (5) Palmer, D. A.; van Eldik, R. *Chem. Rev.* **1983**, *83*, 651–731.
- (6) Yang, X.; Castleman, A. W., Jr. *J. Am. Chem. Soc.* **1991**, *113*, 6766–6771.
- (7) Wang, X.; Conway, W.; Burns, R.; McCann, N.; Maeder, M. *J. Phys. Chem. A* **2010**, *114*, 1734–1740.
- (8) Jönsson, B.; Karlström, G.; Wennerström, H. *J. Am. Chem. Soc.* **1978**, *100*, 1658–1661.
- (9) Liang, J.-Y.; Lipscomb, W. L. *J. Am. Chem. Soc.* **1986**, *108*, 5051–5058.
- (10) Peng, Z.; Merz, K. M., Jr. *J. Am. Chem. Soc.* **1991**, *112*, 2733–2734.
- (11) Peng, Z.; Merz, K. M., Jr. *J. Am. Chem. Soc.* **1993**, *115*, 9640–9647.
- (12) Nemukhin, A. V.; Topol, I. A.; Grigorenko, B. L.; Burt, S. K. *J. Phys. Chem. B* **2002**, *106*, 1734–1740.
- (13) Iida, K.; Yokogawa, D.; Sato, H.; Sakaki, S. *Chem. Phys. Lett.* **2007**, *443*, 264–268.
- (14) Leung, K.; Nielsen, I. M. B.; Kurtz, I. *J. Phys. Chem. B* **2007**, *111*, 4453–4459.
- (15) Tuckerman, M. E.; Marx, D.; Parrinello, M. *Nature* **2002**, *417*, 925–929.
- (16) Marx, D. *ChemPhysChem* **2006**, *7*, 1848–1870.
- (17) Laio, A.; Parrinello, M. *Proc. Natl. Acad. Sci. U.S.A.* **2002**, *99*, 12562–12566. Iannuzzi, M.; Laio, A.; Parrinello, M. *Phys. Rev. Lett.* **2003**, *90*, 238302. Laio, A.; Rodriguez-Fortea, A.; Gervasio, F. L.; Ceccarelli, M.; Parrinello, M. *J. Phys. Chem. B* **2005**, *109*, 6714–6721.

(18) Ensing, B.; Laio, A.; Gervasio, F. L.; Parrinello, M.; Klein, M. *J. Am. Chem. Soc.* **2004**, *126*, 9492–9493. Cucinotta, C. S.; Ruini, A.; Catellani, A.; Stirling, A. *ChemPhysChem* **2006**, *7*, 1229–1234. Stirling, A.; Iannuzzi, M.; Parrinello, M.; Molnar, F.; Bernhart, V.; Luinstra, G. *Organometallics* **2005**, *24*, 2533–2537. Nair, N. N.; Schreiner, E.; Marx, D. *J. Am. Chem. Soc.* **2006**, *128*, 13815–13826. Stanton, C. L.; Kuo, I.-F. W.; Mundy, C. J.; Laino, T.; Houk, K. N. *J. Phys. Chem. B* **2007**, *111*, 12573.

(19) Car, R.; Parrinello, M. *Phys. Rev. Lett.* **1985**, *55*, 2471–2474.

(20) CPMD v3.11. Copyright IBM Corp 1990–2007, Copyright MPI für Festkörperforschung Stuttgart 1997–2001.

(21) Becke, A. D. *Phys. Rev. A* **1988**, *38*, 3098–3100. Lee, C.; Yang, W.; Parr, R. G. *Phys. Rev. B* **1988**, *37*, 785–89.

(22) Laio, A.; Parrinello, M. *Lect. Notes Phys.* **2006**, *707*, 315–347. Laio, A.; Gervasio, F. L. *Rep. Prog. Phys.* **2008**, *71*, 126601.

(23) Stirling, A.; Pápai, I. *J. Phys. Chem. B* **2010**, *114*, 16854–16859.

(24) For the forward runs, we used the following parametrizations for the metadynamics in its Lagrangian formalism: $k_{CV1} = 0.05$; $M_{CV1} = 10.0$; $k_{CV2} = 0.2$; $M_{CV2} = 20.0$; uniform hill heights: 0.5 kcal/mol; widths (in the units of the CVs): 0.4 and 0.1 along CV1 and CV2, respectively. For the backward runs: $k_{CV1} = 5.0$; $M_{CV1} = 100.0$; hill height: 0.3 kcal/mol; hill width: 0.03. The hills have been added at every 120th step (at periods of 20.3 fs).

(25) Park, J. M.; Laio, A.; Iannuzzi, M.; Parrinello, M. *J. Am. Chem. Soc.* **2006**, *128*, 11318–11319.

(26) Leitner, W. *Coord. Chem. Rev.* **1996**, *153*, 257–284.

(27) Since reaction rates are concentration dependent, lowering the pH diminishes the significance of the reaction of CO₂ with OH[−] and increases the rate of the neutral hydrolysis. However, it is difficult to give an accurate theoretical estimation for the pH value where the two rates become equal because the various rate models employ additional parameters (e.g., preexponential in the Arrhenius model, κ in TST, etc.) and it is also not obvious which rate model is applicable for this reaction.

(28) The water oxygens of the first solvation shell can be found at a distance region of 3–3.5 Å from the carbon atom as shown by the partial C–O $g(r)$ function (see, e.g., ref 14).

(29) The number of the coordinating water molecules has been calculated in the following way: first the instantaneous OH[−] ion is identified by the minimum of the following coordination number

$$n_i^H = \sum_{k \in H} \frac{1 - \left(\frac{r_{ik}}{1.4}\right)^{10}}{1 - \left(\frac{r_{ik}}{1.4}\right)^{30}}$$

where i goes over all the oxygen atoms except those of CO₂. Then the number of its coordinating water molecules is calculated by counting the H-bonds which it forms with nearby water molecules. For the presence of a H-bond between the hydroxyl oxygen and the water molecule featuring the j th oxygen, the HB _{j} function is calculated as a product of two terms as given in ref 30

$$HB_j = \frac{1 - \left(\frac{r_j - 2.7}{0.5}\right)^{10}}{1 - \left(\frac{r_{ij} - 2.7}{0.5}\right)^{20}} \sum_k^H \frac{1 - \left(\frac{r_k + r_{jk} - r_j}{0.6}\right)^8}{1 - \left(\frac{r_k + r_{jk} - r_j}{0.6}\right)^{12}}$$

The first term is nonvanishing if the distance r_j between the hydroxyl oxygen and a water O _{j} atom is smaller than 3.5 Å and takes the maximal value 1 when it is around 2.7 Å. In the second term r_k is the distance between the hydroxyl oxygen and the H _{k} atoms, whereas r_{jk} is the distance between O _{j} and H _{k} . The second term is 1 if $r_k + r_{jk} - r_j$ is 0 and gradually vanishes as this sum exceeds 0.6. The coordination number is then given as the sum of these HB _{j} values.

(30) Donadio, D.; Raiteri, P.; Parrinello, M. *J. Phys. Chem. B* **2005**, *109*, 5421–5424.

(31) Ludwig, R. *Angew. Chem., Int. Ed.* **2003**, *42*, 258–260.

(32) Ab initio MD simulations have already demonstrated that hydrated CO₂ exhibits the characteristics of a typical hydrophobic solute.³³

(33) Kumar, P. P.; Kalinichev, A. G.; Kirkpatrick, R. J. *J. Phys. Chem. B* **2009**, *113*, 794–802.